

## Train-induced dynamic behavior analysis of longitudinal girder in cable-stayed bridge

Dong-Hui Yang<sup>1a</sup>, Ting-Hua Yi<sup>\*2</sup>, Hong-Nan Li<sup>1,2b</sup>, Hua Liu<sup>3c</sup> and Tiejun Liu<sup>4d</sup>

<sup>1</sup>School of Civil Engineering, Dalian University of Technology, Dalian 116023, China

<sup>2</sup>School of Civil Engineering, Shenyang Jianzhu University, Shenyang 110168, China

<sup>3</sup>China Railway Major Bridge (Nanjing) Bridge and Tunnel Inspect & Retrofit Co., Ltd., Nanjing 210061, China

<sup>4</sup>School of Civil and Environmental Engineering, Harbin Institute of Technology, Shenzhen 518055, China

(Received December 3, 2017, Revised March 22, 2018, Accepted March 28, 2018)

**Abstract.** The dynamic behaviors of the bridge structures have great effects on the comfortability and safety of running high-speed trains, which can also reflect the structural degradation. This paper aims to reveal the characteristics of the dynamic behaviors induced by train loadings for a combined highway and railway bridge. Monitoring-based analysis of the acceleration and dynamic displacement of the bridge girder is carried out. The effects of train loadings on the vertical acceleration of the bridge girder are analyzed; the spatial variability of the train-induced lateral girder displacement is studied; and statistical analysis has been performed for the daily extreme values of the train-induced girder deflections. It is revealed that there are great time and spatial variabilities for the acceleration induced by train loadings for the combined highway and railway cable-stayed bridge. The daily extreme values of the train-induced girder deflections can be well fitted by the general extreme value distribution.

**Keywords:** railway bridge; structure health monitoring; girder acceleration; dynamic deflection; general extreme value distribution

### 1. Introduction

Normally, train loads are the most important live load for long-span combined highway and railway bridges. Although the self-weight of the bridge structure are dominant for long span bridge, the train load may cause great dynamic impacts on the bridge girder because of the heavy load and high speed, which will induce dynamic behavior of the longitudinal girder and other members of the bridge structures during service life. The train-induced dynamic behaviors involve the periodical deformation and stress cycles which may result in fatigue failure of the structural components and endanger the fatigue life of the bridge. Additionally, the train load-induced impact will cause vibration of the longitudinal girder which has significant effects on the smoothly and safely running of high-speed train (Camara *et al.* 2014). Moreover, the degradation of bridge structural performance during service commonly exists due to environmental and loading actions

(Yang *et al.* 2016), and the dynamic behavior of the bridge structures can also reflect the changes of the structural features, which may be applied to identify the damage of the bridge structures. Therefore, it is necessary to carried out the analysis of the characteristics of train-induced dynamic behavior for combined highway and railway bridges.

The live load-induced dynamic behaviors of the longitudinal bridge girder include the dynamic deflections, strains, velocities, accelerations, etc. Currently, the research on the dynamic behavior of the bridge structures has been carried out by a lot of researchers to analysis the structural dynamic characteristics, detect and located structural damage, evaluate the serviceability and safety of the bridge structures and so on (Ding *et al.* 2016, Huynh *et al.* 2016, Chang and Kim 2016, Türker and Bayraktar 2014). Cantero *et al.* (2017) carried out experimental research on the evolution of bridge modal properties during the passage of a vehicle. They found that the presence of additional frequencies, significant shifts in frequencies and changes in the modes of vibration. Wickramasinghe *et al.* (2016) developed a vibration based damage index to detect and locate damage in suspension bridges. Nagayama *et al.* (2017) proposed a bridge frequency estimation method based on the vehicle-induced vibration. Gia and Goicolea (2017) performed a research on the dynamic vibration of skew bridges due to railway traffic using analytical and simplified models. Cantero *et al.* (2016) studied the effects of vehicle's speed and axle configuration on the responses exited by traversing trains. Moughty and Casas (2017) examined a number of vibration parameters as damage indicator to detect the progressively damage of bridge under

\*Corresponding author, Professor  
E-mail: yth@dlut.edu.cn

<sup>a</sup> Assistant Professor  
E-mail: dhyang@dlut.edu.cn

<sup>b</sup> Professor  
E-mail: hnli@dlut.edu.cn

<sup>c</sup> Ph.D.  
E-mail: kylinbridge@163.com

<sup>d</sup> Professor  
E-mail: liutiejun@hit.edu.cn

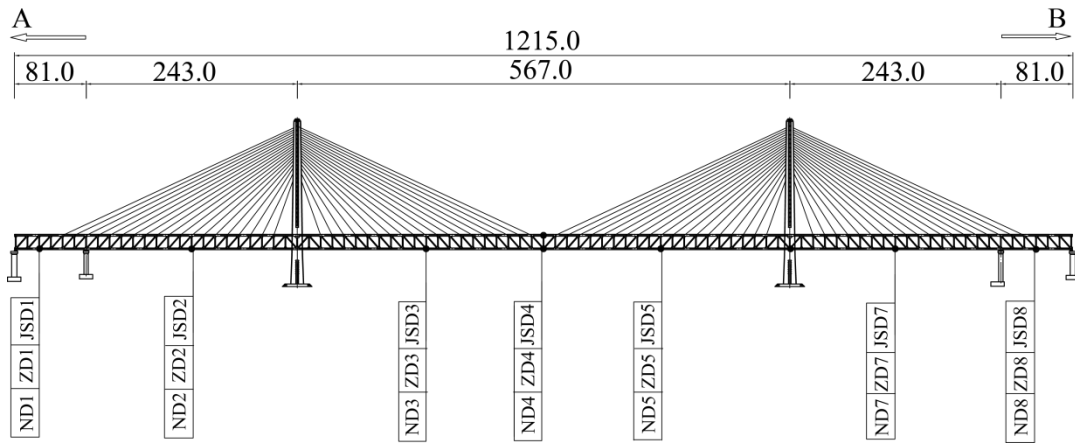


Fig. 1 Sensors placement of the bridge over Yangtze River

ambient excitation. Hong and Park (2015) conducted laboratory experiments on the effects of vehicle-induced vibrations to determine the attainable concrete strength for bridge widening. Podworna (2014) studied the random dynamic behavior of bridges loaded by high-speed train and the effects of vertical track irregularities had been analyzed. Bayraktar *et al.* (2017) carried out dynamic field tests of a long-span cable-stayed bridge and the accelerations of deck, pylons and cables are measured to assess the degradation of the bridge. Plachý *et al.* (2017) also conducted similar dynamic tests to assess an old steel railway bridge by measuring the vertical and horizontal accelerations.

The structural health monitoring (SHM) systems have been applied in many long-span railway bridge projects, which can record the long-term data of structural behavior and reflect the real structural performance during service life. Monitoring-based research on the static and dynamic behavior has attracted great attentions of more and more researchers, which involves the research field of load identification, structural damage detection, performance evaluation, etc (Yi *et al.* 2012a, b, McCullagh *et al.* 2014, Fenerci *et al.* 2017, Ye *et al.* 2018, Ye *et al.* 2013). In this paper, the long term monitoring data of a combined highway and railway cable-stayed bridge have been analyzed to study the train-induced dynamic behavior. The paper has been organized as follows: (1) the combined highway and railway cable-stayed bridge and the SHM system equipped were introduced; (2) the train-induced vertical acceleration of the bridge girder has been studied; (3) the lateral dynamic displacement of the bridge girder is analyzed; and (4) the spatial and time variability of train-induced vertical dynamic displacement of bridge girder were studied and the statistical analysis has been carried out for the daily extreme values for the dynamic displacement.

## 2. Description of bridge and SHM system

The long-term monitoring data of acceleration and dynamic displacement of a bridge over Yangtze River in China were analyzed, which is a long span cable-stayed bridge with three spans and dual towers. The bridge has a symmetric span configuration of  $81.0 + 243.0 + 567.0 +$

$243.0 + 81.0$  m, the mid span of which is 567.0 m and main side span 243.0 m (Fig. 1). The longitudinal girder is fixed with tower and pier at the tower position, and the tensile bearings are used at the side spans to avoid separation between the girder and pier during service. The bridge is a combined highway and railway cable-stayed bridge with the longest span in the world, which makes it slenderer and more flexible than the common simple-supported railway bridges. Moreover, the bridge is subjected high-speed and heavy train load, which may induce great impact on the bridge structure. The enduring live loads and environmental action will cause the degradation of structural performance, which will endanger the structural safety and serviceability. To timely detect and locate the structural damage, a SHM system has been equipped on the bridge to monitor various static and dynamic responses of the bridge in service. The monitoring data of the bridge dynamic behaviors recorded by the SHM systems include the vertical accelerations, lateral and vertical dynamic displacement of bridge girders.

In this paper, the long-term monitoring data of acceleration and dynamic displacement of bridge girder were analyzed, which are recorded by the acceleration sensors and displacement sensors respectively. The locations of the two types of sensors are shown in Fig. 1, and all the deflection sensors are mounted at the upper stream side of the longitudinal girder. The sampling frequency of the vertical dynamic deflection sensors are 1 Hz, while the counterpart of the lateral dynamic displacement sensors is 200 Hz, because the lateral stiffness of bridge girder is larger than vertical direction. Additionally, the sampling frequency of the acceleration sensors is also 200 Hz. The nomenclatures of the sensors are listed in Table 1.

Table 1 Nomenclatures of the sensors of the SHM system

Sensor name	Sensor type	Sampling frequency	Unit
JSD	Acceleration sensor	200 Hz	$\text{mm}/\text{s}^2$
ZD	Lateral displacement sensor	200 Hz	$\text{mm}/\text{s}^2$
ND	Deflection sensor	1 Hz	mm

### 3. Train-induced vertical accelerations of bridge girder

#### 3.1 Variability of acceleration amplitude of longitudinal girder

The bridge is a combined highway and railway cable-stayed bridge, which is subjected to motor vehicles and train loads. The bridge is equipped with acceleration sensors at 7 positions on the longitudinal girder, which are used to monitor the dynamic loading-induced vibration of the bridge girder during the service life. The daily bridge girder acceleration-time curve recorded by sensor JSD4 is plotted in Fig. 2. As shown in Fig. 2, it can be indicated that the acceleration peaks during daytime are dense, while the counterparts recorded at night are relatively sparse.

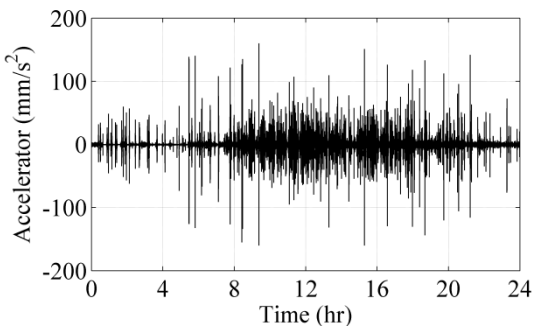


Fig. 2 Acceleration-time curve recorded by JSD1 for January 8th

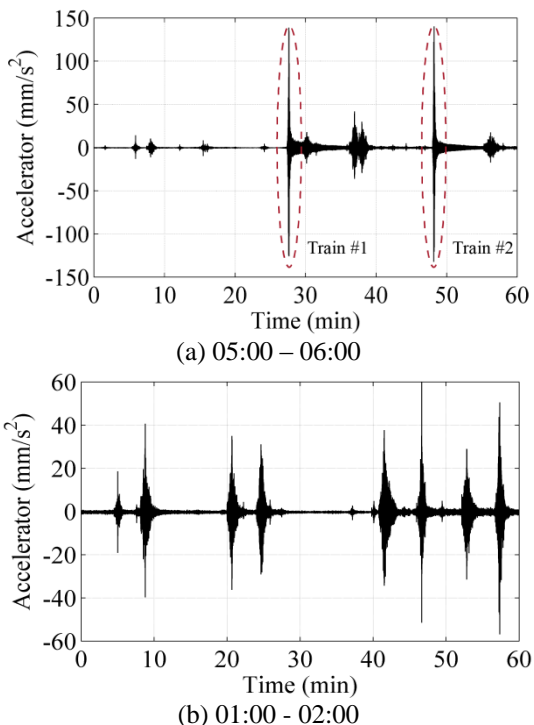


Fig. 3 Hourly acceleration-time curves of JSD1

Considering that the period of 24 hours for the train running schedule, it can be inferred that all the trains pass the bridge during 05:00-22:00 every day. To analyze the differences between the accelerations induced by motor vehicles and trains, the monitoring acceleration data of one hour was further analyzed as presented in Fig. 3. The acceleration data from the time interval of 05:00 – 06:00 was analyzed for train-induced responses (Fig. 3(a)).

Considering that the traffic situation at night is less complex than daytime, the acceleration data from 01:00 – 02:00 was selected to analyze the motor vehicle induced dynamic behavior of the bridge girder (Fig. 3(b)), which can avoid the aliasing of the dynamic responses caused by different passing vehicles. As shown in Fig. 3(a), there are two obvious acceleration peaks induced by two passing trains, the amplitudes of which reached 140 mm. The relative small acceleration signals are evenly distributed in the other regions of the curve. By contrast, several similar acceleration peaks exist in the curves in Fig. 3(b), which are induced by motor vehicles, and the amplitudes are all less than 60 mm, which are much less than the train-induced ones.

#### 3.2 Spatial variation of bridge girder acceleration induced by train

To study the train-induced acceleration at the different positions of the longitudinal bridge girder, the monitoring acceleration data from the JSD1 and JSD8 are further analyzed (Fig. 4). As presented in Fig. 3(a), there are two trains passing the bridge during 05:00 – 06:00. Therefore, it can be inferred that the acceleration peaks in Fig. 3 are also caused by the two trains. The acceleration amplitudes of the auxiliary span girder induced by trains and motor vehicles are similar to each other, which is different from the situation of mid span girder. As for JSD8, some motor-induced acceleration amplitudes are even larger than the counterparts induced by trains, which can be attributed to the larger stiffness of the girder enhanced by the short span.

By comparing the sequence of the occurrence of the acceleration peaks recorded by JSD1 and JSD8 induced by the same train load, the running direction of the train can be identified. The first train ran from A side to B side because the acceleration peak was first recorded by JSD1 (Fig. 4). Similarly, the second train ran from B side to A side for the acceleration peak first recorded by JSD8. Taking the girder acceleration at the auxiliary span as example, the effects of train running direction on the characteristics of the bridge girder acceleration are analyzed. As shown in Fig. 5, the acceleration amplitude induced by the train at JSD1 is 72.1 mm/s<sup>2</sup>, and the counterpart at JSD8 is 91.0 mm/s<sup>2</sup>. The acceleration amplitudes at the two auxiliary spans induced by the same train are relatively close to each other, which indicates a symmetry of the bridge structures along the longitudinal direction. Additionally, the evolution process of the acceleration responses at the two auxiliary spans has also been analyzed. For the auxiliary span girder at A side, the train-induced acceleration increases rapidly to the maximum value and then declines gradually to zero. By contrast, the amplitude of the train-induced acceleration at

B side increases gradually to the maximum and then rapidly decreases to zero. The developing processes at the two auxiliary spans are quite different because the train has been on the bridge before running by JSD8, while the bridge has not been subjected to train load before the train ran by JSD1.

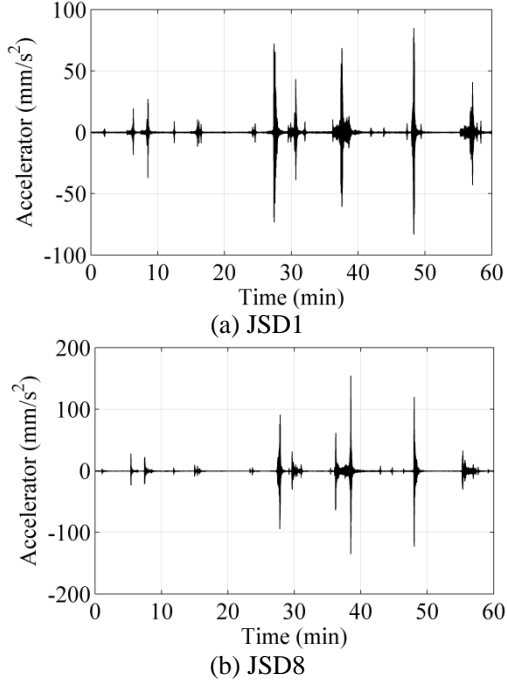


Fig. 4 Acceleration responses of auxiliary span girder at 05:00-06:00

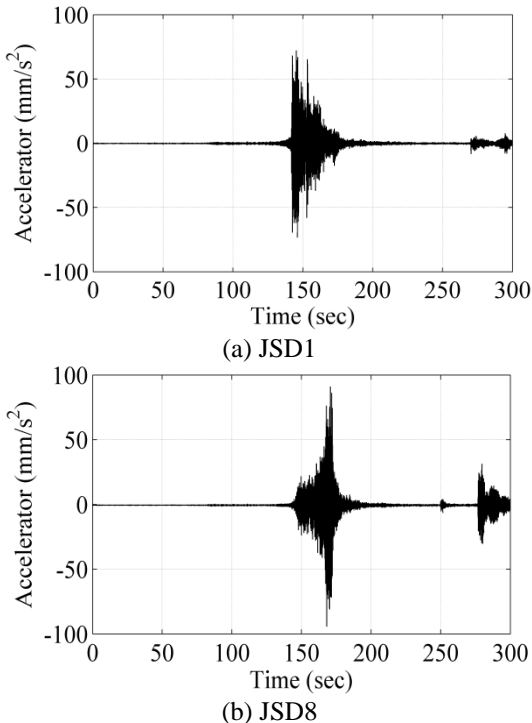


Fig. 5 Acceleration of bridge girder induced by the first train

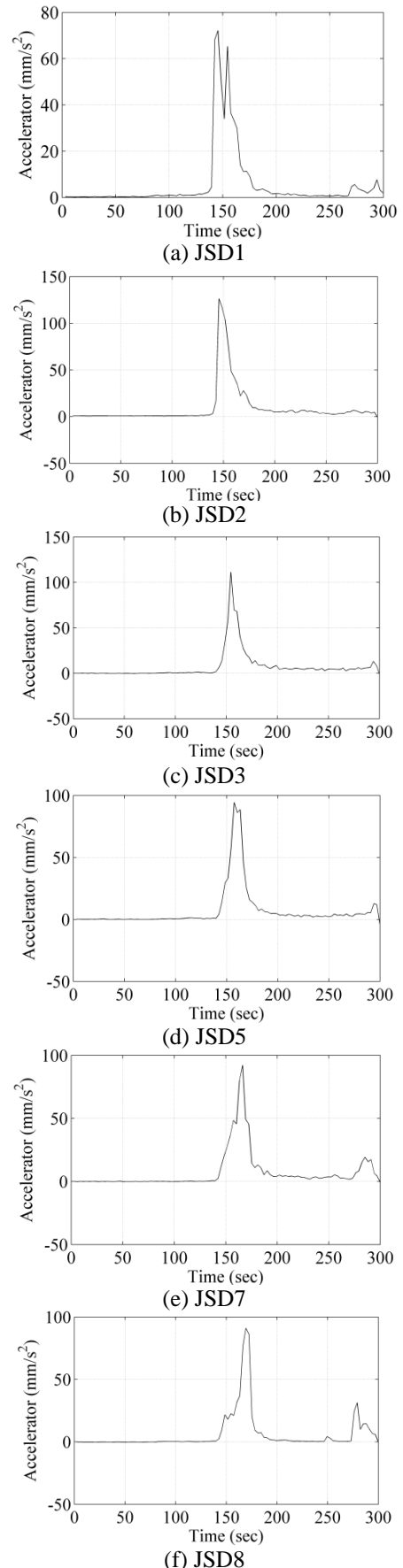


Fig. 6 Envelop diagram of girder acceleration amplitude

Table 2 Train-induced vertical acceleration amplitude of bridge girder ( $\text{mm/s}^2$ )

Train No.	JSD1	JSD2	JSD3	JSD4	JSD5	JSD7	JSD8
#1	73.3	122.3	107.4	132.3	99.8	106.4	92.7
#2	84.9	126.3	136.9	136.2	98.5	160.2	127.3
#3	98.4	114.2	113.9	99.4	109.3	125.2	98.7
#4	72.7	146.7	92.9	124.1	104.5	112.3	116.6

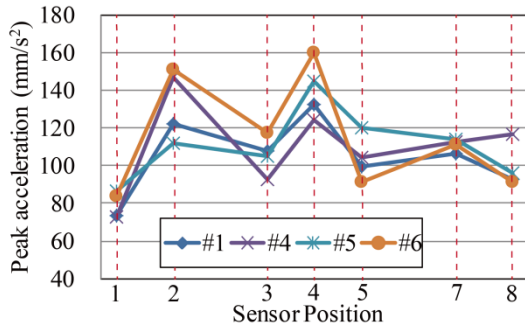


Fig. 7 Variation of bridge girder acceleration amplitude along longitudinal direction

The envelopes of the acceleration at different girder positions induced by the first train are plotted in Fig. 6. As for the JSD1 section at A side where the train first ran by, an obviously acceleration peak occurred at the very beginning. For JSD2 section, the acceleration peak gradually moves to the right side of the envelop diagram and the amplitude of the acceleration peak also increases. When the train crosses JSD3 and JSD5 at the mid span, the acceleration peaks nearly locate at the middle of the envelop diagram. When the train passes JSD7, the acceleration peak moves to the right side of the envelop diagram. When the train runs by the position of JSD8 at the auxiliary span, the acceleration peak moves to the extreme right side and then decreases rapidly to zero.

When the same train crosses the bridge, there are great differences between the train-induced acceleration amplitudes at the different positions of the bridge girder along the longitudinal directions. To study the variability of the train-induced acceleration amplitudes along the bridge longitudinal direction, the monitored vertical girder acceleration data from 05:00 – 10:00 are analyzed. The preliminary analysis of the monitoring data reveals that there are 6 trains passing the bridge during that time. The correlation between the acceleration amplitudes at different positions along the longitudinal direction was analyzed. The maximum values monitored acceleration peaks at the 7 positions of the girder are listed in Table 2.

It can be further revealed by Fig. 7 that the vertical acceleration of the bridge girder induced by different trains varies similar along the longitudinal direction. For the same train, the induced acceleration amplitude at the side span is larger than the auxiliary span, and the acceleration peak value at the middle of mid span are larger than the other positions of the mid span.

#### 4. Train-induced lateral dynamic displacement of bridge girder

The lateral dynamic displacement of the bridge girder under the impact of trains or motor vehicles can reflect the lateral dynamic feature of the girder. The monitoring data of the lateral dynamic girder displacement at ZD1 and ZD4 in January 8th were analyzed, which are shown in Fig. 8. It is indicated that the maximum value of the lateral dynamic displacement of the auxiliary span is larger than that in mid span. Furthermore, three one-hour acceleration-time curves recorded ZD4 are specified in Fig. 9, which represent the three typical time intervals of a day. Comparing Figs. 9(a) and (b), the peaks of the lateral dynamic girder displacements at daytime are denser than night time. Therefore, the lateral dynamic displacement of the girder can be attributed to the impact of trains and motor vehicle loadings. In order to reduce the interference of the environmental actions and avoid the superposition of the dynamic responses caused by different live loading in complex traffic condition, the monitoring data of lateral girder displacement between 01:00 – 02:00 was analyzed. As shown in Fig. 9(a), seven obvious peaks of dynamic displacement can be observed, which coincide with the counterparts of the girder acceleration (Fig. 3(b)). Additionally, a comparison between Fig. 9(b) and Fig. 3(a) is further conducted, which shows that two peaks of the dynamic displacement coincide with the counterparts of bridge girder acceleration peaks. Consequently, the lateral girder dynamic displacement is mainly caused by impacts of the vehicle and train loadings. Besides, the amplitude of the lateral dynamic displacement induced by trains is similar to motor vehicles for mid span girder, but larger than motor vehicles for auxiliary span girder of the bridge.

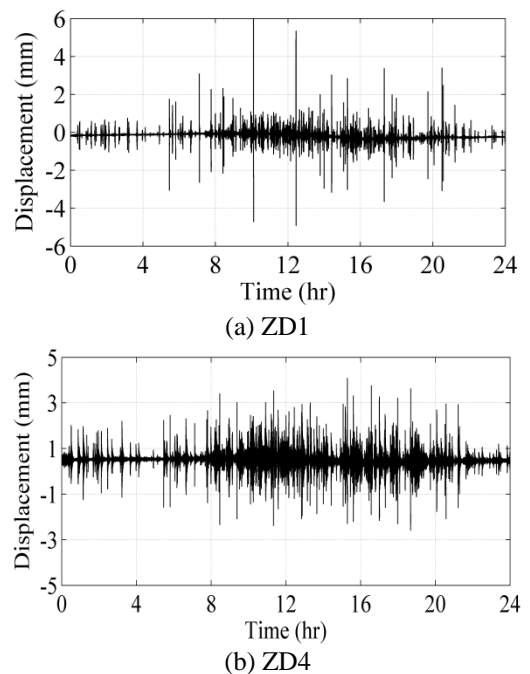


Fig. 8 Daily monitoring data of dynamic lateral displacement of the bridge girder

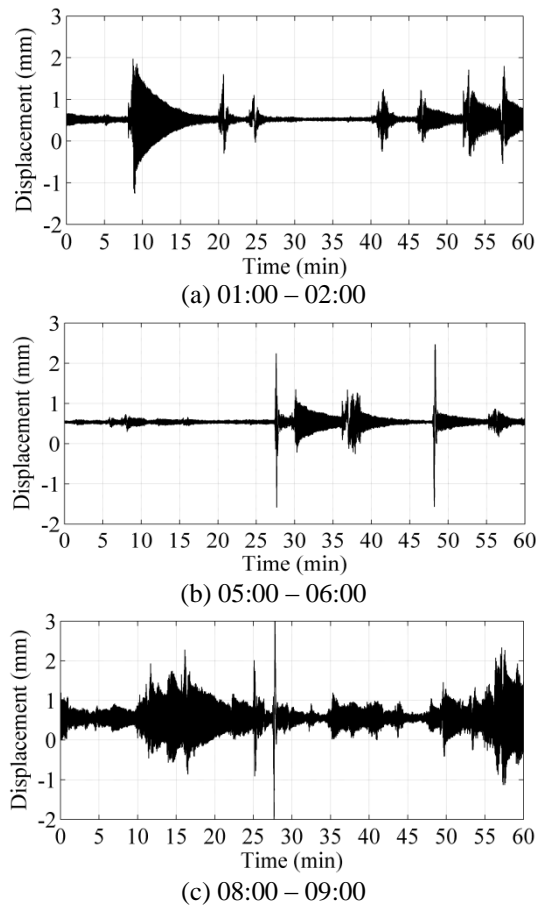


Fig. 9 Hourly lateral girder displacement

## 5. Train-induced dynamic deflection of bridge girder

### 5.1 Variability of dynamic girder deflection

Because the bridge structure is subjected to the trains, temperature and other external actions, the dynamic deflection of the bridge girder is a time-dependent value. The bridge girder deflections can reflect the features of structural stiffness, which have substantial effects on the comfortability and safety of the high-speed trains passing through the bridges. Therefore, it is necessary to study the variability of the dynamic deflections of the bridge girder. In order to identify the train-induced dynamic deflections, two days of monitored displacement data, January 1st and 8th, are analyzed respectively. As indicated in Fig. 10, the deflection peaks with the amplitude over 20mm always occurred at the same time in the two days. Because the running schedule of the train is relatively stable and there is obvious randomness for the motor vehicles on the bridges, it can be inferred that the deflection peaks over 20 mm are caused by trains. As shown in Fig. 10, there are also many small peaks distributed on the deflection-time curves other than the train-induced ones. Additionally, sine-like variation trend can also be observed in the deflection-time curve. As reported by the other research work of the authors, the sine-like variation of the curve is caused by the temperature actions and the small peaks are caused by random vehicle

loadings. To study the characteristics of the train-induced girder deflections, it is essential to eliminate the effects of the temperature actions and the motor vehicle loadings.

Compared with the effects of the train and motor vehicle loadings, the temperature-induced girder deflection varies slowly with time, which can be considered to be a kind of low frequency-field signal. Therefore, wavelet frequency decomposition method was applied to abstract the low-frequency ingredient from the initial recorded signal. The mother wavelet function of db6 was applied and 10-layer decomposing scale was selected. As shown in Fig. 11(a), the static deflection induced by temperature was obtained through the wavelet frequency decomposition method, which has a close correlation with the overall trend of the raw data. Therefore, the deflections induced by live loads can be obtained by subtracting the temperature-induced effects. Considering the amplitudes of the train-induced deflections are obviously larger than the motor vehicles, the train-induced deflections can be further acquired by subtracting the small peaks of the deflections.

Through the process above, the train-induced dynamic girder deflections can be obtained for auxiliary, side and mid span. The train-induced deflections at ND1 and ND2 are presented in Fig. 12. It can be observed that the train caused greater deflection in side span than auxiliary span, and both of them are smaller than the mid span (Fig. 11(b)), which can be attributed to the auxiliary span being stiffer than side span because of the shorter span length. Additionally, the features of the dynamic deflections induced by train loadings at different positions are quite different.

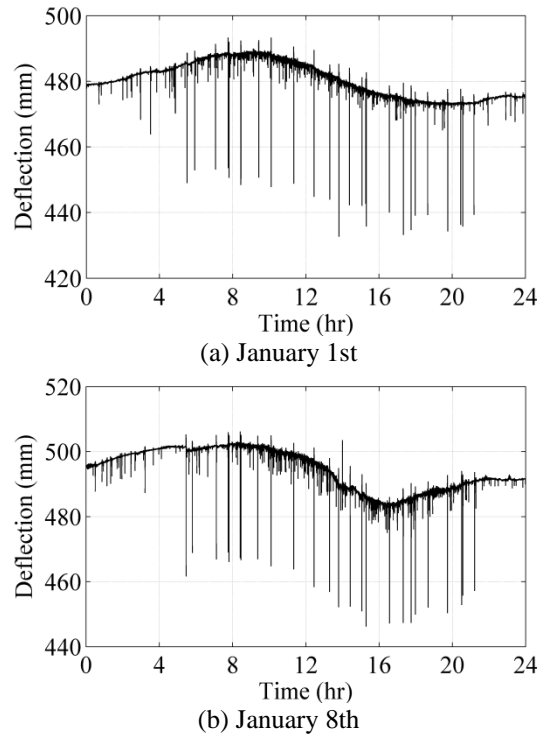


Fig. 10 Vertical dynamic displacement of bridge girder at ND4

For auxiliary and side span girder, the amplitudes of upward and downward dynamic deflection peaks are similar to each other. However, the downward deflection amplitudes at mid span girder are much larger than the upward ones. Considering that the girder deflections could reflect the comprehensive effects of the static and dynamic effect of the train loadings, the extreme values, mean values and root square mean (RSM) values of the train-induced girder deflection amplitudes are calculated for the bridge girder, which are shown in Fig. 13. It can be observed that the absolute values of the three statistical parameters are larger at mid span than the side and auxiliary span.

### 5.2 Statistical analysis of train-induced dynamic girder deflection

For high-speed railway bridge, the amplitude of the girder dynamic deflection can affect the irregularity of the track, which could substantially endanger the running safety and comfortability of the high-speed trains. Therefore, it is essential to carry out a long-term monitoring of the girder deflections and statistically analyze the monitoring data, which is meaningful for engineering practice. In this section, the time-variation of the extreme values of the train-induced girder deflections are studied. Based on the results concluded in section 5.1, the daily extreme values of the girder dynamic deflections are caused by trains, which are shown in Fig. 11.

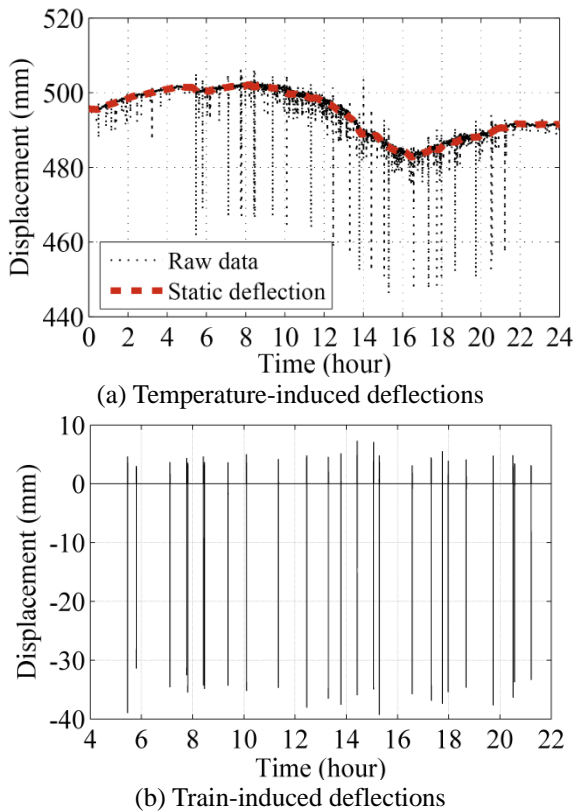


Fig. 11 Dynamic deflection-time curves at ND4 in January 8th

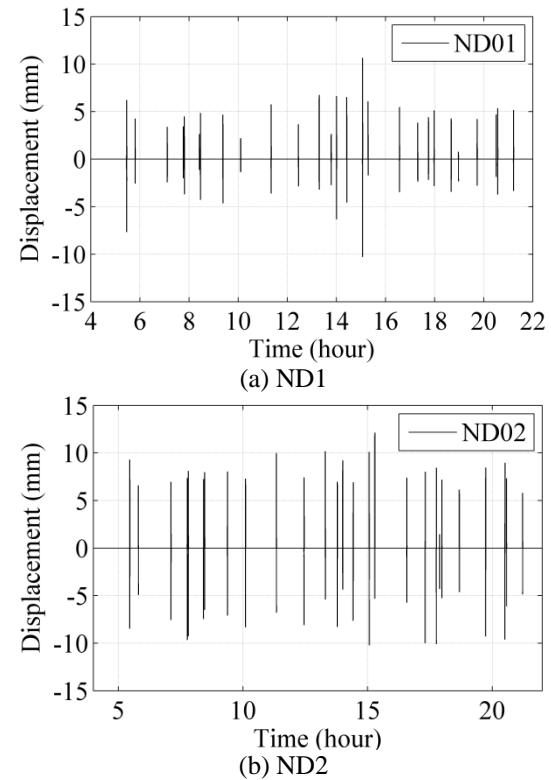


Fig. 12 Train-induced dynamic deflection-time curve in January 8th

Although the extreme values of the dynamic girder deflections are mainly attributed to the train loadings, the bridge girder is also subjected to wind actions, random vehicle loadings, etc. Moreover, the train loading is variable with the different carrying loads. Consequently, the variability of the train loads and other external actions will make the dynamic girder deflection a random variable rather than a constant. As shown in Fig. 11(b), the amplitudes of train-induced girder deflections are similar to each other; however, obvious randomness exists. Therefore, it is necessary to carry out statistical analysis of the daily extreme values of the girder deflections.

To analyze the statistical characteristics of the dynamic girder deflection, the relatively complete monitoring data of the train-induced dynamic girder deflections from May to September in 2015 were selected for analysis. Because the running schedule of the train has a period of 24 hours, the daily extreme values of the dynamic girder deflection induced by the train loadings are statistically analyzed. The histogram of the daily extreme values of dynamic girder deflections for ND1, ND2, ND3 and ND5 are plotted in Fig. 14. It can be observed that most samples of the extreme values of the train-induced girder deflections gather at the region of relative small values, while few samples are sparsely distributed at the region of large values. According to the distribution features above of the dynamic deflections, general extreme value (GEV) distribution is adopted to fit the probability density function of the extreme values of the dynamic girder deflections. GEV distribution is developed within extreme value theory which consists of a family of three continuous probability

distributions, namely the Gumbel, Fréchet and Weibull distributions. The PDF of GEV can be represented as Eq. (1).

$$f(x; \sigma, \xi, \mu) = \begin{cases} \frac{1}{\sigma} \left(1 + \xi \frac{x - \mu}{\sigma}\right)^{(-1/\xi)-1} \exp\left[-\left(1 + \xi \frac{x - \mu}{\sigma}\right)^{-1/\xi}\right] & \xi \neq 0 \\ \frac{1}{\sigma} \exp\left(-\frac{x - \mu}{\sigma}\right) \exp\left[-\exp\left(-\frac{x - \mu}{\sigma}\right)\right] & \xi = 0 \end{cases} \quad (1)$$

where  $\sigma > 0$  is the scale parameter;  $\mu \in \mathbf{R}$  is the location parameter;  $\xi \in \mathbf{R}$  is the shape parameter;  $x$  is the random variable. The sub-families of the GEV distribution can be defined by  $\xi = 0$ ,  $\xi > 0$  and  $\xi < 0$ , which correspond to the Gumbel, Fréchet and Weibull distributions respectively. It is worth noting that the PDF is always positive. Thus for  $\xi > 0$ , the Eq. (1) is valid for  $x > -\sigma / \xi + \mu$ , while for  $\xi < 0$ , it is valid for  $x < -\sigma / \xi + \mu$ .

When GEV distribution is applied to fit the dynamic girder deflection, the unknown parameters consist of  $\sigma$ ,  $\mu$  and  $\xi$ , which need to be determined through the monitoring samples of the daily extreme values of the deflections. The maximum likelihood estimation (MLE) method is used to estimate the parameters of the PDF in Eq. (1). The likelihood function can be represented as Eq. (2),

$$L(\boldsymbol{\theta}; x_1, \dots, x_n) = \prod_{i=1}^n f(x_i; \boldsymbol{\theta}) = P(X_1 = x_1, \dots, X_n = x_n | \boldsymbol{\theta}) \quad (2)$$

where  $\boldsymbol{\theta}$  is the vector the unknown parameters of the PDF of GEV distribution.  $x_i$  is the  $i$ th independent observation of the random variables.  $P(\cdot)$  is the conditional probability of the observed  $x_i$  given  $\boldsymbol{\theta}$ . The mechanism of MLE method is to maximize the probability of the occurrence of the observed values of  $x_1, x_2, \dots, x_n$  under the condition of  $\boldsymbol{\theta}$ . The MLE can be represented as Eq. (3).

$$L(\hat{\boldsymbol{\theta}}; x_1, \dots, x_n) = \max_{\boldsymbol{\theta} \in \Theta} L(\boldsymbol{\theta}; x_1, \dots, x_n) \quad (3)$$

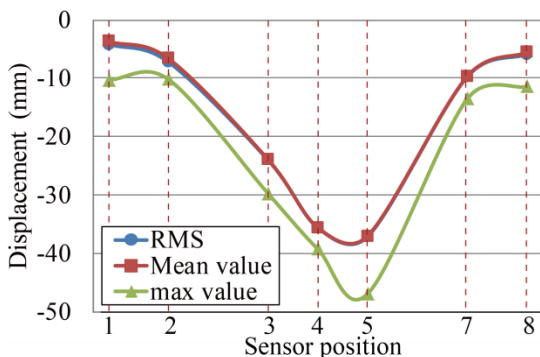


Fig. 13 Spatial variation of train-induced dynamic girder deflection

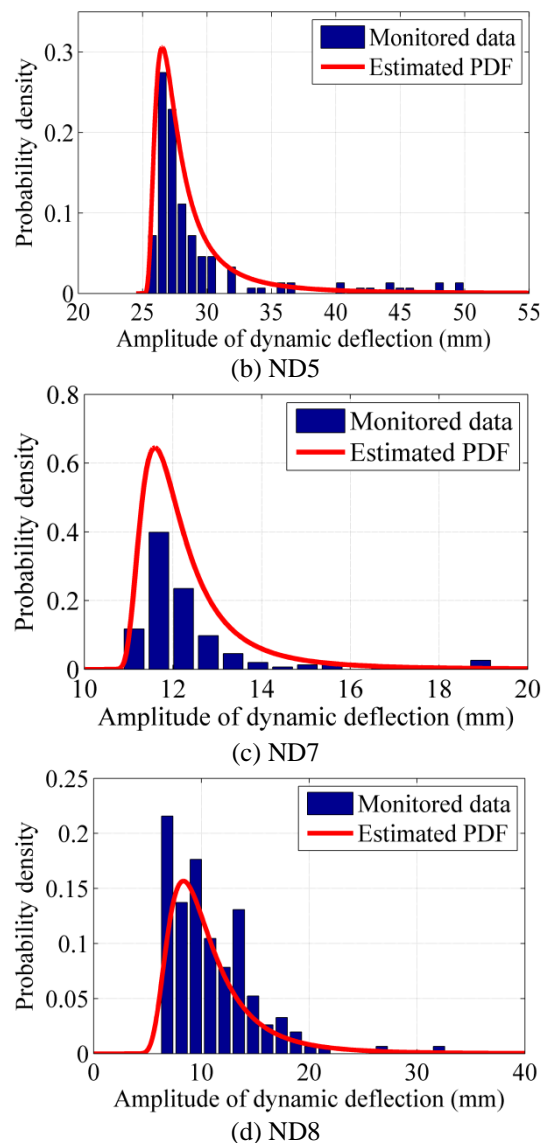
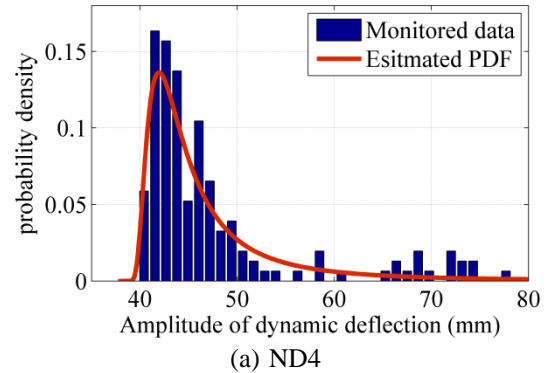


Fig. 14 Daily extreme values of dynamic girder deflections

where  $\hat{\boldsymbol{\theta}}$  is the maximum likelihood estimator. Considering  $L(\boldsymbol{\theta}; x_1, \dots, x_n)$  reaches the maximum value at the same points with  $\ln(L(\boldsymbol{\theta}; x_1, \dots, x_n))$ ,  $\hat{\boldsymbol{\theta}}$  can be obtained through Eq. (4) to simplify the calculation.

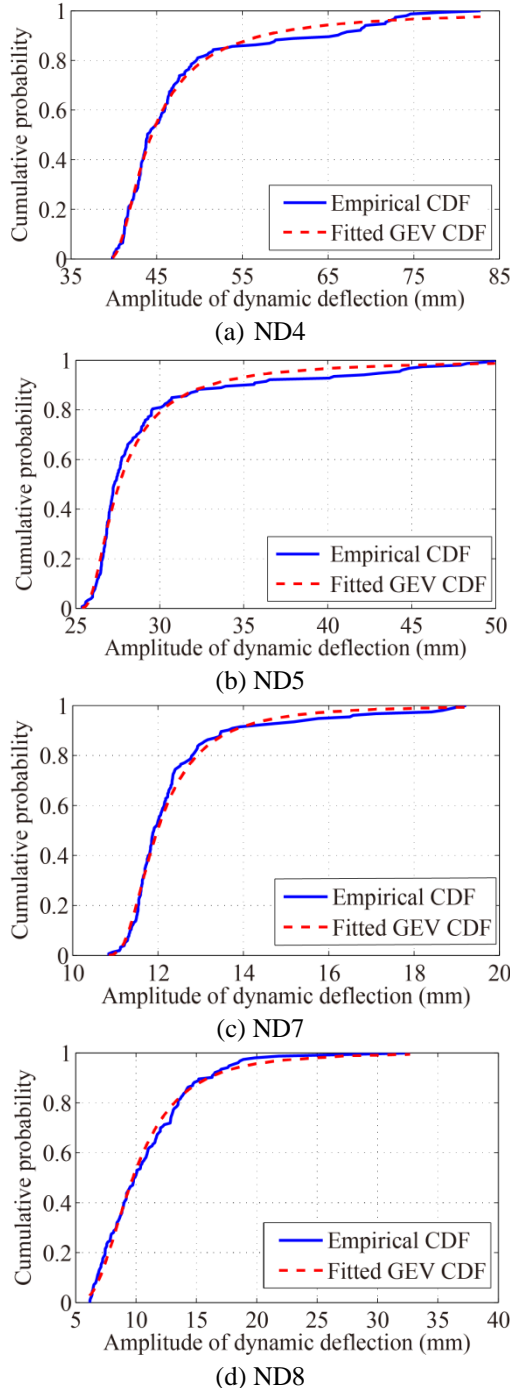


Fig. 15 CDF of daily extreme values of dynamic girder deflections

$$\frac{\partial}{\partial \theta_j} \ln(L(\boldsymbol{\theta}; x_1, \dots, x_n)) = 0 \quad (4)$$

Based on the monitoring data, the PDF of the dynamic girder deflections of four typical cross sections of the girder have been fitted by GEV distribution, which are shown in Fig. 14. The PDF parameters of the GEV distribution have been obtained through MLE, which are listed in Table 3. As shown in Fig. 14, the observed samples of the extreme values of the dynamic girder deflections can be well

fitted by the GEV distribution, and the monitoring data of mid span girder is better fitted than side span. To quantitatively evaluate the validity of the fitting results, Kolmogorov–Smirnov test (*K*-*S* test) was applied and the test results are listed in Table 4. It is worth noting that the threshold values of significant level are the limit values beyond which the *K*-*S* test will reject the GEV distribution hypothesis. According to the testing results, the significant level of daily deflection extreme values at ND4 failing to reject the GEV distribution hypothesis can reach 74%, with the counterparts at ND5, ND7 and ND8 are 0.31, 0.40 and 0.45. It can be further concluded that the train-induced daily extreme girder deflection at mid span can be better fitted by GEV distribution than the other spans. The empirical cumulative distribution function (CDF) curves obtained based on the monitoring data and the fitted GEV CDF obtained through MLE are plotted in Fig. 15. It can be observed that the fitted GEV CDF coincides well with the empirical CDF, which indicates that it is reasonable for the daily extreme values of the train-induced bridge girder deflection to approximately obey the GEV distribution.

## 6. Conclusions

The bridge girder accelerations and dynamic displacements can be induced by trains, motor vehicles and ambient environmental actions. The structural dynamic behaviors can reflect the dynamic features of the bridge structure, which have been more and more widely applied to detect structural damage and evaluate the structural performance degradation. Train loads are the most important live loads for long-span combined highway and railway bridges. Although the train loads are much smaller than the self-weight of the bridge structure, the dynamic responses of the bridge are mainly attributed to the impact of the train loadings. Therefore, it is necessary to study the characteristics and variability of the train-induced dynamic behaviors of the bridge. In this paper, the monitoring data of a combined highway and railway cable-stayed bridge was analyzed to study the features of the train-induced bridge girder dynamic responses in service.

Table 3 Maximum likelihood estimators of the GEV PDF parameters

Deflection position	$\xi$	$\sigma$	$\mu$
ND4	0.57	3.10	43.17
ND5	0.53	1.36	27.04
ND7	0.33	0.60	11.75
ND8	0.24	2.41	8.83

Table 4 Threshold values of significant level

Significant level	ND4	ND5	ND7	ND8
$\alpha_{thr}$	0.74	0.31	0.40	0.45

Firstly, the accelerations of the bridge girder were analyzed based on the monitoring data, and the differences between the acceleration amplitudes induced by train and vehicles were analyzed; Secondly, the differences between the propagation processes of the girder acceleration for the different girder positions were studied; thirdly, the spatial variability was revealed for the train-induced lateral girder displacement. Finally, the method was proposed for subtracting the effects of temperature and vehicle loadings on dynamic girder deflections, and statistical analyses were carried out for the daily extreme values of the train-induced girder deflections. The following conclusion can be drawn:

- Both of the vehicle and train loadings can cause vertical accelerations in bridge girder in combined highway and railway cable-stayed bridge. For the mid span girder, the amplitudes of the girder acceleration induced by trains are obviously larger than vehicle loadings. By contrast, the train-induced acceleration of auxiliary and side span girder approximates to that induced by vehicles.
- There is a close correlation between the propagation process of the vertical girder accelerations and the train running directions for the auxiliary span girders. For the auxiliary span at the starting point of the train running direction, the acceleration rapidly increases to the peak. For the auxiliary span at the other side, it will take a relatively long time for the acceleration to reach the peak. Additionally, the train-induced vertical girder acceleration peak at auxiliary span is smaller than the side span, and the counterpart of the mid span section is larger than that of the quarter span section in the mid span girder.
- The lateral girder displacements are mainly attributed to train and vehicle loadings. The train-induced lateral displacement amplitude approximates to that induced by vehicles at the mid span. However, the train-induced lateral girder displacement is obviously larger than the vehicles for auxiliary span girder.
- Wavelet frequency decomposition method can be effectively used to eliminate the effects of temperature actions on the girder deflections and abstract the train-induced girder deflections. The daily extreme values, mean values and the RMS values of the girder deflection increase with the positions from auxiliary span to the mid span.

• There is obvious randomness in daily extreme values of the girder deflections induced by trains. The distribution of the daily extreme values of the girder deflection for the mid span can be well fitted by the GEV distribution model, and the parameters of the GEV PDF can be obtained through the MLE method. *K-S* test further verifies that the monitoring data of the daily extreme girder deflections induced by trains do not reject the GEV distribution.

## Acknowledgements

The writers gratefully acknowledge the sponsorship of the National Natural Science Foundation of China (Grant Nos. 51708088 & 51625802), the 973 Program (Grant No.

2015CB060000), the National Key Research and Development Program of China (Grant No. 2016YFC0701108), and the China Postdoctoral Science Foundation (Grant No. 2017M611224).

## References

- Bayraktar, A., Türker, T., Tadla, J., Kurşun, A. and Erdiş, A. (2017), "Static and dynamic field load testing of the long span Nissibi cable-stayed bridge", *Soil Dyn. Earthq. Eng.*, **94**, 136-157.
- Camara, A., Nguyen, K., Ruiz-Teran, A.M., and Stafford, P.J. (2014), "Serviceability limit state of vibrations in under-deck cable-stayed bridges accounting for vehicle-structure interaction", *Eng. Struct.*, **61**, 61-72.
- Cantero, D., Hester, D. and Brownjohn, J. (2017), "Evolution of bridge frequencies and modes of vibration during truck passage", *Eng. Struct.*, **152**, 452-464.
- Cantero, D., Ülker-Kaustell, M. and Karoumi, R. (2016), "Time - frequency analysis of railway bridge response in forced vibration", *Mech. Syst. Signal Pr.*, **76-77**, 518-530.
- Chang, K., and Kim, C. (2016), "Modal-parameter identification and vibration-based damage detection of a damaged steel truss bridge", *Eng. Struct.*, **122**, 156-173.
- Ding, Y.L., Zhao, H.W., Li, A.Q. (2017), "Temperature effects on strain influence lines and dynamic load factors in a steel truss arch rail way bridge using adaptive fir filtering", *J. Perform. Constr. Fac.*, 10.1061/(ASCE)CF.1943-5509.0001026. 10-1061.
- Fenerci, A., Øiseth, O. and Rønnquist, A. (2017), "Long-term monitoring of wind field characteristics and dynamic response of a long-span suspension bridge in complex terrain", *Eng. Struct.*, **147**, 269-284.
- Gia, K.N. and Goicoeal, J.M. (2017), "Vibration analysis of short skew bridges due to railway traffic using analytical and simplified models", *Procedia EngineeringX International Conference on Structural Dynamics, EURODYN 2017*, **199**, 3039-3046.
- Hong, S. and Park, S. (2015), "Effect of vehicle-induced vibrations on early-age concrete during bridge widening", *Constr. Build. Mater.*, **77**, 179-186.
- Huynh, T., Park, J. and Kim, J. (2016) "Structural identification of cable-stayed bridge under back-to-back typhoons by wireless vibration monitoring", *Measurement*, **88**: 385-401.
- McCullagh, J.J., Galchev, T., Peterson, R.L., Gordenker, R., Zhang, Y., Lynch, J. and Najafi, K. (2014), "Long-term testing of a vibration harvesting system for the structural health monitoring of bridges", *Sensor. Actuat. A: Phys.*, **217**, 139-150.
- Moughty, J.J. and Casas, J.R. (2017), "Performance assessment of vibration parameters as damage indicators for bridge structures under ambient excitation", *Procedia EngineeringX International Conference on Structural Dynamics, EURODYN 2017*, **199**, 1970-1975.
- Nagayama, T., Rekswardojo, A.P., Su, D. and Mizutani, T. (2017), "Bridge natural frequency estimation by extracting the common vibration component from the responses of two vehicles", *Eng. Struct.*, **150**, 821-829.
- Plachý, T., Polák, M. and Ryjáček, P. (2017), "Assessment of an old Steel railway bridge using dynamic tests", *Procedia EngineeringX International Conference on Structural Dynamics, EURODYN 2017*, **199**: 3053-3058.
- Podworna, M. (2014), "Vibrations of bridge / track Structure / high-speed train system with vertical irregularities of the railway track", *Procedia EngineeringXXIII R-S-P Seminar; Theoretical Foundation of Civil Engineering (23RSP) (TFoCE 2014)*, **91**, 148-153.
- Türker, T. and Bayraktar, A. (2014), "Structural safety assessment

- of bowstring type RC arch bridges using ambient vibration testing and finite element model calibration”, *Measurement*, **58**: 33-45.
- Wickramasinghe, W.R., Thambiratnam, D.P., Chan, T.H.T. and Nguyen, T. (2016), “Vibration characteristics and damage detection in a suspension bridge”, *J. Sound Vib.*, **375**, 254-274.
- Yang, D.H., Li, G.P., Yi, T.H. and Li, H.N. (2016), “A performance-based service life design method for reinforced concrete structures under chloride environment”, *Constr. Build. Mater.*, **124**, 453-461.
- Ye, X.W., Ni, Y.Q., Wai, T.T., Wong, K.Y., Zhang, X.M. and Xu, F. (2013), “A vision-based system for dynamic displacement measurement of long-span bridges: algorithm and verification”, *Smart Struct. Syst.*, **12**(3-4), 363-379.
- Ye, X.W., Xi, P.S., Su, Y.H., Chen, B. and Han, J.P. (2018), “Stochastic characterization of wind field characteristics of an arch bridge instrumented with structural health monitoring system”, *Struct. Saf.*, **71**, 47-56.
- Yi, T.H., Li, H.N. and Gu, M. (2012a), “Sensor placement for structural health monitoring of Canton Tower”, *Smart Struct. Syst.*, **10**(4-5), 313-329.
- Yi, T.H., Li, H.N. and Zhang, X.D. (2012b), “Sensor placement on Canton Tower for health monitoring using asynchronous-climb monkey algorithm”, *Smart Mater. Struct.*, **21**(12), Article ID: 125023.